

Geothermal Reconnaissance Study for Sinai Peninsula, Egypt

Gad El-Qady^{1,2}, Ahmed Salem³, Essam Aboud², Ahmed Khalil² and Keisuke Ushijima²

1-National Research Institute of Astronomy and Geophysics (NRIAG), 11722 Helwan, Cairo, Egypt

2-Erath resources department, Kyushu University, 6-10-1 Hakozaki, Fukuoka 812-8581 Japan

3- Airborne geophysical dept., Nuclear Material Authority of Egypt, Maadi, Egypt.

gad@mine.kyushu-u.ac.jp

Keywords: Sinai, Geophysics

ABSTRACT

Sinai Peninsula is characterized by superficial thermal manifestations represented by a cluster of hot springs with varied temperatures (30-72°C). These springs are mostly issue out of fractures and distributed along the Eastern shore of the Gulf of Suez. In this work, we present a reconnaissance study to elucidate the geothermal resources and delineate the structural setting of the area using available geophysical data; including heat flow, geothermal logs, geoelectrical resistivity and aeromagnetic data. The heat flow and geothermal well logging measurements showed that the eastern part of the peninsula is characterized by a high heat flow with an average value of 70mW/m². Geoelectrical resistivity surveys were conducted in terms of Vertical Electrical Soundings (VES) at some localities nearby the surface thermal manifestations. The resulted geoelectrical cross sections delineated the subsurface structure at the studied localities and gave an explanation for the hot water source. Interpretation of magnetic data indicated that the hot springs in the western side of the peninsula are structurally controlled. Additionally, the calculated depth to Curie point isotherm ranges between 6.2 and 19.7 Km. Generally, the results indicate that Sinai Peninsula is a promising for further geothermal exploration.

1. INTRODUCTION:

Sinai Peninsula is one of the main geographic units of Egypt and represents the Asiatic part of Egypt. Sinai Peninsula, covering an area of some 61000 km², is triangular in shape and separated geographically from the Eastern Desert by the Gulf of Suez (Fig.1). It is considered as unstable shelf due to the frequent earthquake activities and its relation with the geologic setting of the area, which is controlled by the tectonic activity of the Red sea, Gulf of Suez and Gulf of Aqaba. Additionally, Sinai area is characterized by superficial thermal manifestations represented by a cluster of hot springs with varying temperatures (35-72°C). These springs are mostly issue out of fractures and distributed along the eastern shore of the Gulf of Suez. Several studies addressed the geologic and tectonic setting of Sinai area (e.g. Said, 1962, Omara, 1972, and Said 1990). However the geothermal studies were not enough to elucidate the geothermal regime of Sinai. Most of these studies (e.g. Swanberg et al., 1983) are concentrated, mainly, on the groundwater geothermometry that was restricted only to the surface hot springs. Some other studies were based on oil well temperature data and its relevance to hydrocarbon exploration (e.g. Tewfic, 1975).

In an attempt to study the possible geothermal sources in Sinai area and to help characterize the geothermal setting of

Sinai Peninsula, we estimated the depths to the Curie-point isotherm based on spectral analysis of the aeromagnetic data. In addition, DC resistivity surveys were conducted at three localities in the vicinity of thermal hot springs, to elucidate the possible aquifer. Some available information from borehole temperatures is used to enhance the results of the geophysical interpretation.

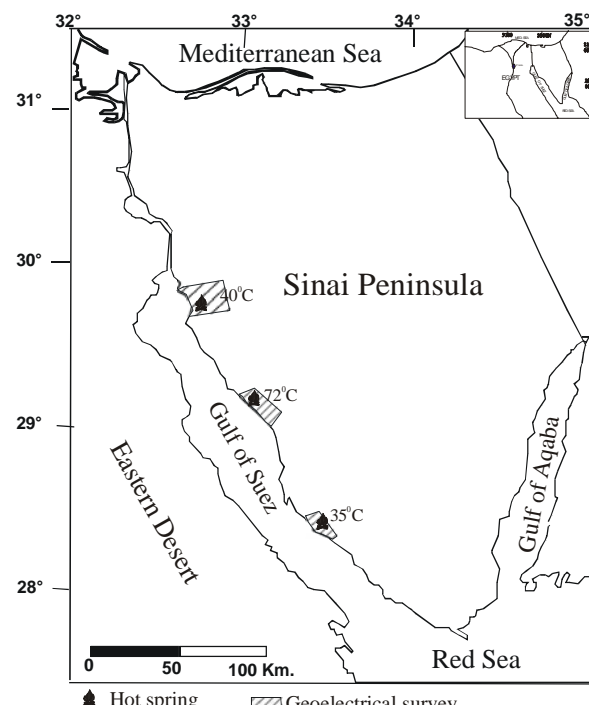


Figure 1: Location map of Sinai area. Hot springs, its surface water temperature and the geoelectrical survey location are displayed.

2. GEOLOGIC REGIME

Sinai Peninsula is the most fascinating region from the geological stand points of view because it displays a variety of simple and complex structural forms, (Abu Al-Izz, 1971). In general, Sinai reflects in miniature all geologic column of Egypt.

Geomorphologically, Sinai Peninsula comprises seven geomorphologic districts. Among these seven districts, the southern elevated mountains district occupies the southern part of Sinai assuming a triangular shape with its apex at Ras Mohamed to the south. The central plateau district occupies the central part of Sinai Peninsula in the form of two main questas; El Egma to the southwest, and El Tieh to the north (Abu Al-Izz, 1971), while the Hilly district lies to the northeast of Sinai Peninsula. It is gently sloping towards

the northeast and is characterized by local isolated hills. In addition, a coastal district of gently undulated surface marked by sand ridges of thick sandstones. While muddy and marshy land district occupies the shorelines and some lakes (e.g. El Bardawel, El Temsah and Bitter lakes) were established.

Figure (2) shows the main surface geologic units at Sinai. For instant, the Paleozoic rocks were suggested for beds overlying the Precambrian basement in the southwestern Sinai (Omara, 1972, and Kora, 1995). The Mesozoic strata crops out in northern Sinai where an almost complete sequence from Triassic to Cretaceous is known, (Kerdany and Cherif, 1990), while it composes a subsurface section attaining a very huge thickness (955 m for Jurassic rocks only) at Ayun Musa.

One of the most important Mesozoic rock units is the Nubian sandstone of lower cretaceous which represent the main water bearing unit in the region. It attains a maximum thickness of about 500 m, while at central Sinai it is made up of 70-130 m. (Kora, 1995) While among the Cenozoic rocks, we find that Oligocene is the most important from the geothermal point of view. The end of the Oligocene period witnessed the rifting movements that brought the Gulf of Suez to its modern shape. Along the numerous faults that crossed the region, simatic molten material climbed up and appears in the form of sporadic but frequent lava flows, sills, sheets and dike feeders chiefly of olivine basaltic and olivine diabase.

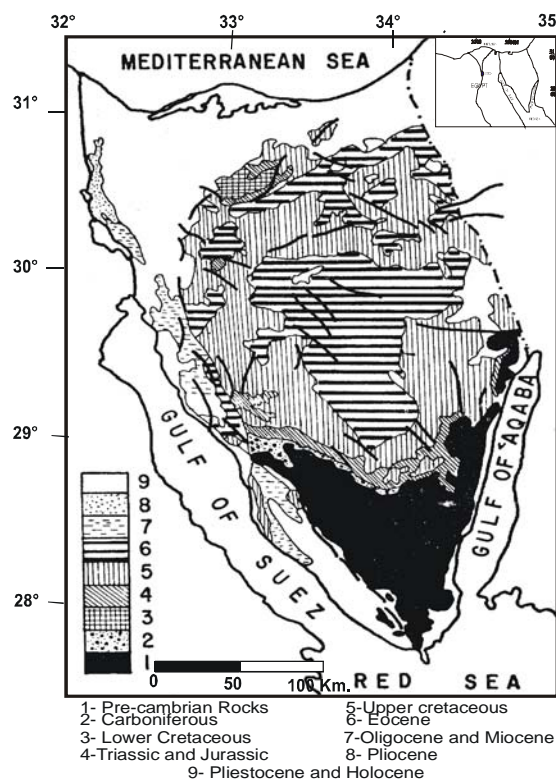


Figure 2: the main surface geologic units at Sinai

Structurally, many workers (e.g. Ball, 1916; Moon and sadek, 1921; Shata, 1956 Abu Al-Izz, 1971 and El-Shinnawi and Sultan, 1973,) had addressed the structure of Sinai, which falls into seven structural regions. Among of these and which is in our concern is the south Sinai shield area, which occupies the southern portion of Sinai and is composed essentially of igneous and metamorphic complex. Also, there is a group of small NE-SW folds each

less than five kilometers long, cross the major folds. There is also an area of faults extends to the north of latitude 30° N for a distance of 200 Km from east to west. In addition, there is a narrow elongated plain extending along the western border of Sinai in NW-SE direction and is characterized by the presence of a series of normal faults of varying lengths and displacements. Almost all of these faults are oriented in the NW-SE direction parallel to the Gulf of Suez composing west Sinai rift area.

3. GEOTHERMAL REGIME OF SINAI:

The geothermal regime of Sinai is illustrated in this study by two means, thermal surface manifestations and heat flow patterns. The surface thermal manifestation in Sinai area is represented only in three hot springs, Ayun Musa, Hammam Pharaoun and Hammam Mousa at El Tor which are located on the eastern shore of the Gulf of Suez (Fig. 1). The surface water temperature in these springs varies from 35 up to 72 °C. These springs owe their existence to tectonic heating associated with the opening of the Red Sea / Gulf of Suez rift (Boulos, 1990). However, it is an indication of a geothermal potentiality in the area.

As for heat flow, there is a minor boreholes devoted mainly for heat flow studies (e.g. Fig. 3, at Ayun Musa area) where the heat flow patterns of Sinai is estimated, in addition to oil well. However, the eastern margin of the crystalline Sinai massif is characterized by the highest heat flow values of more than 90mW/m² (Fig. 4). While for the western margin along the Gulf of Suez, assuming thermal conductivity of 2.3 W/mK as a minimum value, the heat flow was estimated to be 60-80mW/m² but may attain as much as 100 mW/m² (Morgan et al., 1977; Boulos et al., 1990). Taking into account the presence of a thick evaporates section of high conductivity in the Gulf of Suez section; these values have to be multiplied. The thermo-mechanics process controlling the tectonic evolution of the Gulf of Suez is still enigmatic. However, the anomalously large size of the rift flank for the amount of extension at the Gulf of Suez suggests a thermal uplift component (Stickler, 1985; Feinstein et al., 1996).

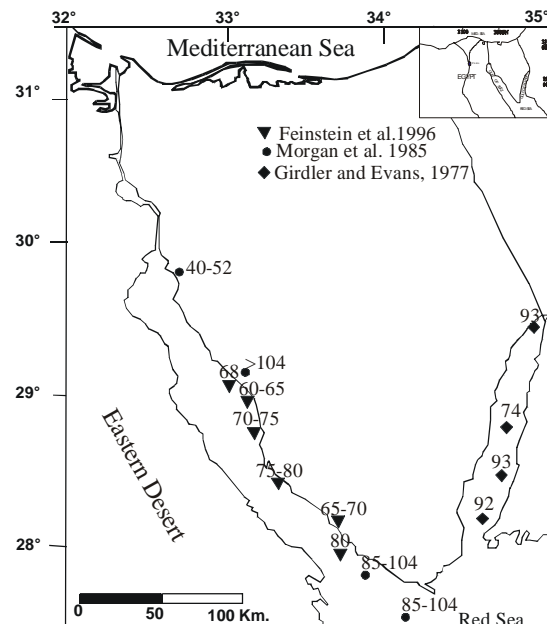


Figure 3: Heat flow values (mw/m²) in Sinai and vicinity.

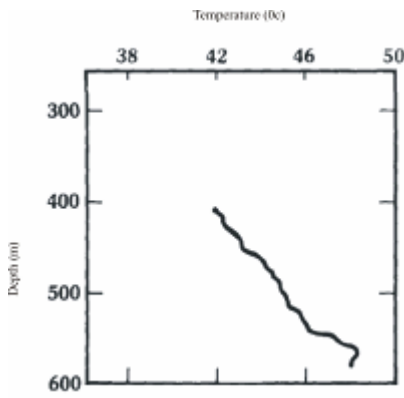


Figure 4: Temperature-depth plot for Ayun Musa BH-1 well (Modified after Morgan et al., 1985).

4. AEROMAGNETIC DATA:

Sinai area was covered by an aeromagnetic survey with a flight elevation of 300 m above the sea level (see references in Ghazala, 1994). The northern part of the map area (Fig. 5) is characterized by elongated magnetic anomalies trending in the E-W direction which could be related to the Ragabet El-Naam E-W shear zone (Ghazala, 1994). Other circular anomalies are observed and could be interpreted as uplifting basement or intrusion of dibasic dykes. The southern part of the map shows also several circular magnetic anomalies that could be related to strike-slip movements of the Gulf of Aqaba (Ben Avraham et al., 1985). In this study, the magnetic data are interpreted using Euler method (Reid et al., 1990) and the depth to Curie point was estimated using spectral analysis approach (Salem, et al., 2000).

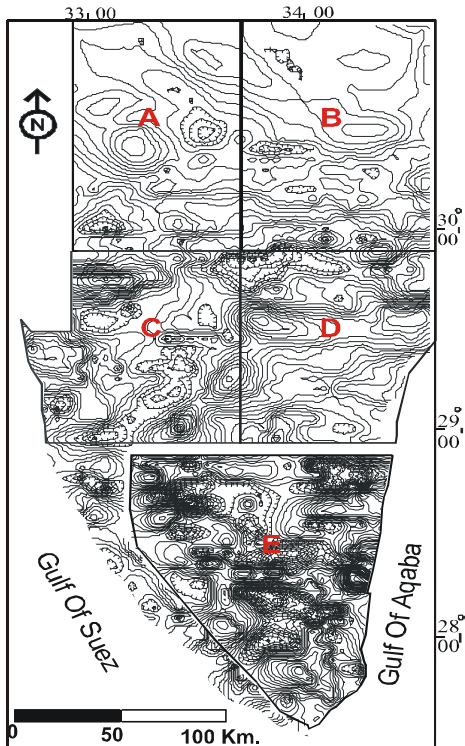


Figure 5: Aeromagnetic map of Sinai area.

4.1. Euler Deconvolution:

The 3D form of Euler's equation can be defined (Reid et al., 1990) as:

$$x \frac{\partial T}{\partial x} + y \frac{\partial T}{\partial y} + z \frac{\partial T}{\partial z} + \eta T = x_o \frac{\partial T}{\partial x} + y_o \frac{\partial T}{\partial y} + z_o \frac{\partial T}{\partial z} + \eta b, \quad (1)$$

where x , y and z are the coordinates of a measuring point, x_o , y_o , and z_o are the coordinates of the source location, b is a base level, and η is a structural index defining the anomaly attenuation rate at the observation location (e.g., $\eta = 0$ for a contact, $\eta = 1$ for the top of a vertical dike or the edge of a sill, $\eta = 2$ for the center of a horizontal or vertical cylinder, and $\eta = 3$ for the center of a magnetic sphere or a dipole, (Thompson, 1982; Reid et al., 1990). By considering four or more neighboring observations at a time (an operated window), source location (x_o, y_o, z_o) and b can be computed by solving a linear system of equations generated from equation (1). In the present study, we have separated the magnetic data and the Euler approach is applied to both residual and regional components. A value of 0.5 was selected as a structural index to locate the possible magnetic contacts from the regional and residual magnetic data. Theoretically, a structural index of zero is an appropriate value for contact models. However, this value usually gives unstable results (Barbosa et al., 1999). Figures 6 and 7 show the Euler solutions for the regional and residual data, respectively. Good clustering of the solutions was obtained and showing definite magnetic trends. The solutions show several trends (E-W, NW-SE, NE-SW, and N-S) and having a depths ranged between 2.5 and 8.0 km. Geologically, Sinai area is considered to be a major tectonic province controlled by trends of the Red Sea, Gulf of Suez and Gulf of Aqaba rifts (Abu El Izz, 1971). These major tectonic features could be observed on Figure 6. The most dominant trend in Figure 7 is the E-W trend. Ben-Avraham (1971) has recognized that the E-W shear zone (Ragabet El-Naam) acting as a front for the Syrian Arc structures.

4.2 Spectral analysis

The idea of using aeromagnetic data to estimate Curie-point isotherm depth is not new, many authors have addressed (e.g. Battacharyya and Leu, 1975; Byerly and Stolt, 1977; Shuey et al., 1977; Connard et al., 1983; Okuba et al., 1985 and Salem et al., 2000). Estimates of the thickness of the magnetized portion of the earth's crust suggest that there are two types of lower boundaries of the layer of the magnetized rocks. The first type of boundary corresponds to vertical changes in crustal composition. The second type is where high temperatures at depth cause the rocks to lose their ferromagnetic properties i.e., below the Curie-point isotherm depth (Connard et al., 1983). The studied area is believed to be consistent with the second type. In this work, we attempt to estimate the depth to Curie point based on spectral analysis using the same method as Salem et al. (2000). When a significant spectral maximum does occur, indicating that the source bottoms are detectable, the frequency f_{\max} of the spectral peak, the mean depth h to the source tops and the mean depth d to the source bottom are related by

$$f_{\max} = \frac{1}{2\pi(d-h)} \ln \frac{d}{h} \quad (2)$$

We have divided the study area into 5 grids (Labeled A, B, C, D and E on Figure 5). For each grid, power spectrum was calculated and depth to the Curie point was estimated (Table 1). Figure 8 shows an example of radially power spectrum for the grid C.

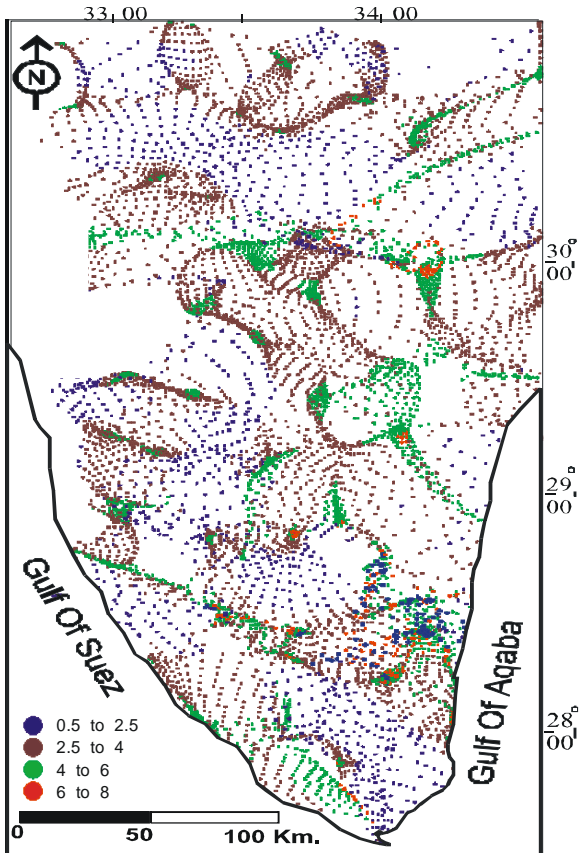


Figure 6: Solutions of Euler method obtained from regional magnetic data.

5. GEOELECTRICAL RESISTIVITY DATA:

The geoelectrical resistivity survey described in this work has been carried out by DC resistivity sounding with Schlumberger array. Three areas had been surveyed to delineate the aquifer around the thermal hot springs (Fig.1). We preferably selected those three distinct areas due to the thermal surface manifestations represented by the hot springs at those areas. The surveys aimed at ascertaining the vertical distribution of water-bearing zones, constituting the aquifer bodies in the region.

5.1. Ayun Musa area:

At the first locality in the vicinity of Ayun Musa (Mousse's springs), Fig. (9), a number of 19 VES stations were measured, using electrode spacing started from $AB/2 = 2$ up to 1000 m, in a successive steps. The field sites were chosen on the basis of the accessibility and applicability of the Schlumberger method.

The VES resistivity data were initially processed in an iterative 1-D modeling technique proposed by Zohdy (1989). The final model derived by Zohdy technique was then taken, in combination with a simple resistivity-depth transformation of the observed data, as an initial model for routine 1-D inversion (Meju, 1994).

A selective example of this process (VES no. 12) is shown in Fig (10). The digitized field curve is given at Fig. (10-a), meanwhile, the final model from inversion and the geologic interpretation are portrayed in Figure (10-b). Inspection of the calculated VES's curves reveals that, the number of the interpreted layers is varying from four to six layers through the study area. For better understanding of the hydrogeology of Ayun Musa area, VES data coupled with

the available borehole inventory are carried out. It revealed that the resistivity values are mainly governed by the lithological units. This illustrated that the Miocene deposits (Marl, sandstone, and limestone) are distinguished by varying resistivity attaining a value up to 150 Ohm.m. Additionally, the main water aquifer is representing by Nubian sandstone at depth starts from 300 m.

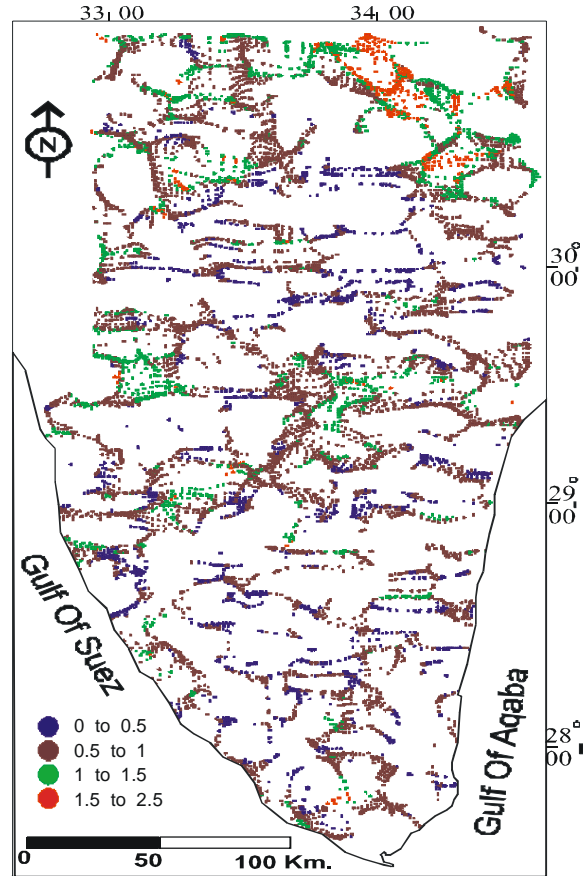


Figure 7: Solutions of Euler method obtained from residual magnetic data.

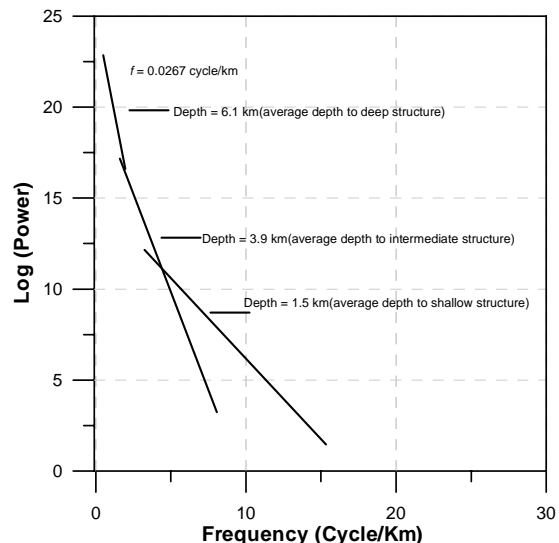


Figure 8: Example of average power spectrum of aeromagnetic anomaly map for the grid C.

Table (1) Results of spectral analysis and depth estimations for the grids A, B, C, D and E

Grid	Spectral peak (Cycle/km)	Shallow sources	
		Depth to the top (km)	Depth to the bottom*(km)
A	0.022	2	18
B	0.020	2	20
C	0.026	4	11
D	0.025	2	14
E	0.041	3	6

* Depth to Curie point

5.2. Hammam Faraun area:

At Hammam Faraun area, El-Qady et al, (2000) have described a geoelectrical resistivity survey compromised of 17 VES using the same parameters of the survey at Ayun Musa area. They came to conclusion that, the 2-D resistivity interpretation of the VES data provides valuable information about the subsurface structure which is differentiated into two main faulting systems in NNW-SSE and E-W directions. That gives explanation for the origin of the hot water, which is deep circulation along the fault plain. Additionally, a huge thick aquifer (~100 m) in the vicinity of the hot spring was elucidated. A promising area for geothermal drilling around the Hammam Faraun hot spring was recommended. Fortunately, nowadays, a project for exploiting this hot water for medical purposes has been started.

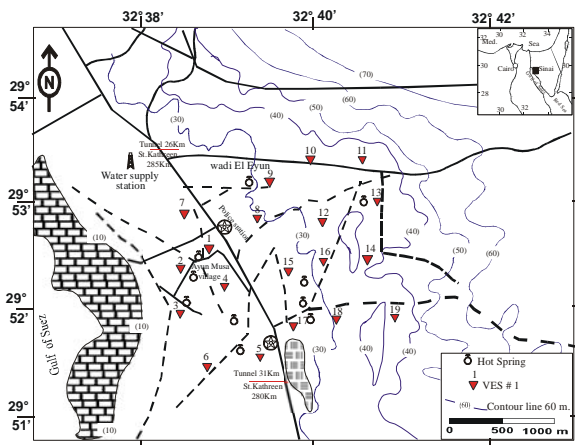


Figure 9: Location map of DC resistivity survey at Ayun Musa hot springs.

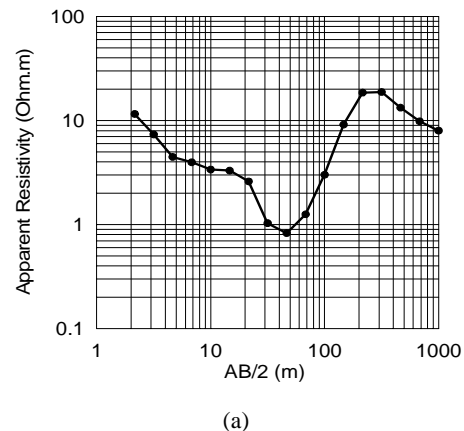
5.3. Hammam Mousa area:

Far away to the south at the vicinity of El-Tor city, the capital town of Southern Sinai, Hammam Mousa spring was located (Fig.1). A DC resistivity survey was conducted in terms of 19 VES using the same parameters of the above two surveys. The survey was devoted to map the aquifer of the area as well as delineate the possible subsurface structure that may have a relation with the hot spring system. The VES data had been inverted into 2-D using ABIC dependent algorithm (El-Qady et al., 1999, and Uchida 1991). According to the results obtained through the inversion process, we could be able to construct the 2-D

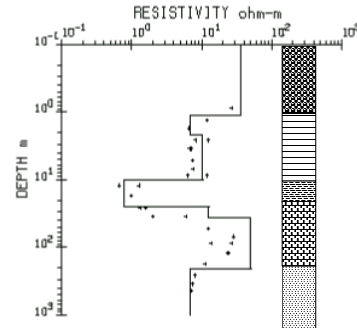
geoelectrical section for the surveyed area. Fig.(11) portrays the cross section of the inverted 2-D model after the fifth iteration for the profile (A-A') running through the hot spring. The initial model is assumed to be 100 ohm.m homogenous earth and the topography is incorporated into the model. The number of the observed data used for the inversion process is 144 while the number of resistivity blocks is 88. At VES No.1, there is a thick low resistivity zone which might be correlated with the hot water saturated zone. Additionally, a fault system is affecting the section, which favoring the issuing of hot water in this place.

6. CONCLUSION:

The present study aimed to reconnoiter the geothermal setting at Sinai Peninsula using the available geophysical data, mainly magnetic and DC resistivity. Sinai Peninsula is characterized by high heat flow patterns that has values more than 100 mW/m², specially the southern part and along Gulf of Aqaba.



(a)



(b)

Figure 10: Example One- dimensional modeling results for VES 12 at Ayun Musa area. (a) Observed data curve. (b) Interpretation using Meju technique

Interpretation of aeromagnetic data was done using the Euler method for the regional and residual data. Good clustering of the solutions obtained show several trends which are trending in E-W, NW-SE, NE-SW, and N-S directions and depths range from 2.5 to 8.0 km. However, the most dominant trend is the E-W trend which acts as a front for the Syrian Arc structures at Sinai area.

Additionally, the magnetic map of the study area has been divided into five grids to estimate the depth to Curie point isotherm. The depths of Curie point have values varying from 6.2 to 19.7 km. That means that the geothermal source is very shallow compared with other regions in Egypt, like Red Sea - the most high heat flow pattern.

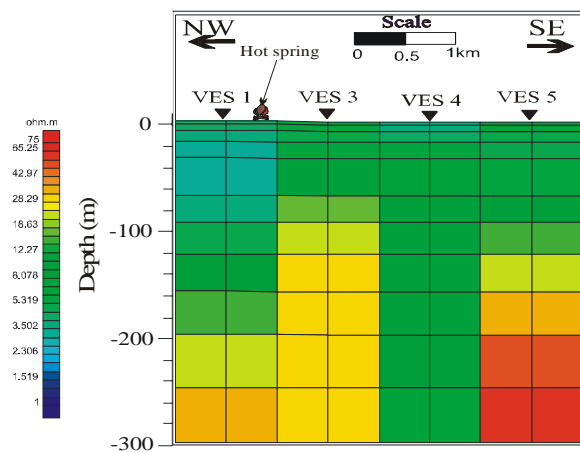


Figure 11: the 2-D geoelectrical cross section along profile A-A'.

Detailed geoelectrical survey at the three localities having thermal surface manifestations could elucidate the groundwater aquifer which is the main source of hot water in the vicinity of the hot springs. At Ayun Musa area, the water aquifer of Miocene is located around 300 meter depth, which is very reasonable for exploitation. Meanwhile, at Hammam Faraun hot spring, the aquifer is little deeper and more thick. At the three localities, the 2-D geoelectrical cross sections elucidates and give a reasonable explanation to the hypothesis of the origin of hot water sources at the hot springs. The hypothesis stated that, the hot water is deeply circulated and comes to the surface through the fault plains at the hot springs area.

As a recommendation, deep geophysical surveys using electromagnetic techniques are highly recommended to elucidate the deep seated structure at the hot springs area. This also will enlighten more information about the real situation and subsurface follow of the hot water.

7. ACKNOWLEDGEMENT:

The authors would like to express their sincere thanks to the National Research Institute of Astronomy and Geophysics (NRIAG), Egypt, for the facilities required for data acquisition in this work. Sincere thanks to all the staff of Exploration Geophysics Lab in Kyushu University for their support during this work. We appreciate the thoughtful comments made by the anonymous reviewers that improved the paper. Efforts and support of the technical program committee are highly appreciated. The work of GE is supported by the Japan Society for the Promotion of Science (JSPS).

8. REFERENCES:

- Abu Al-Izz, M.S. 1971. Landforms of Egypt. 281p. Dar A1-Maaref, Cairo, Egypt.
- Ball, J., 1916: The geography and geology of west-central Sinai, Egypt. Survey Dept., Cairo, 1-219.
- Barbosa, V. C. F., Silva, J. B. C., and Mederios, W. E., 1999, Stability analysis and improvement of structure index estimation in Euler deconvolution, *Geophysics*, 64, 48-60.
- Ben-Avraham, Z.O. 1985. Structural framework of the Gulf of Elat (Aqaba), Northern Red Sea. *Geophysical Research* 90, 703-726.
- Bhattacharyya, B. K., and Leu, L.K. (1975). Analysis of magnetic anomalies over Yellowstone National Park. Mapping the Curie-point isotherm surface for geothermal reconnaissance. *J. Geophys. Res.*, Vol.80, pp.461-465.
- Boulos, F., 1990: Some aspects of the geophysical regime of Egypt in relation to heat flow, groundwater and microearthquakes. In: Said R., 1990 (ed.): the geology of Egypt. 407-438, Balkema, Rotterdam.
- Byerly, P.E., and Stolt, R.H. (1977). An attempt to define the Curie point isotherm in northern and central Arizona. *Geophysics*, Vol.42, pp.1394-1400.
- Connard, G., Couch, R., and Gemperle, M. (1983). Analysis of Aeromagnetic measurements from the Cascade Range in central Oregon. *Geophysics*, Vol.48, pp.376-390.
- El-Qady G., Sakamoto, C. and Ushijima, K., 1999: 2-D inversion of VES data at Saqqara archaeological area, Egypt. *Earth Planets and Space*, 51, 1091-1098.
- El-Qady, G., Ushijima, K., and El-Sayed A., 2000: Delineation of a geothermal reservoir by 2D inversion of resistivity data at Hammam Faraun area, Sinai, Egypt. Proceeding World Geothermal Congress. 1103-1108.
- El-Shinnawi M.A and Sultan, I., 1973: Lithostratigraphy of some subsurface upper cretaceous sections in the Gulf of Suez area, Egypt, *Acta Geol. Hungaria*, Vol., 17, 469-493.
- Feinstein, S., Kohn, B., Steckler M., and Eyal, M., 1996: Thermal history of the eastern margin of the Gulf of Suez, I. Reconstructed from borehole temperature and organic maturity measurements. *Tectonophysics*, 266, 203-220.
- Ghazala, H., 1994: Structural interpretation of the Bouguer and aeromagnetic anomalies in central Sinai. *Journal of African Earth Sciences*, V. 19, pp. 35-42
- Girdler, R.W. and T.R. Evans, 1977: Red Sea heat flow. *Geophys. J. the Roy. Astr. Soc.*, Vol.51, pp.245-251.
- Kerdany, M., and Cherif, O., 1990: Mesozoic. In: Said R., 1990 (ed.): the geology of Egypt. 407-438, Balkema, Rotterdam.
- Kora, M., 1995: An introduction to the stratigraphy of Egypt. Lecture notes, Geology Dept. Mansoura Univ., 116pp.
- Meju, M., 1994, Geophysical data analysis: Understanding inverse problem theory and practice, SEG Course Notes Series, V. 6, 296 p.
- Moon, F., Sadek, H., 1921: Topography and geology of northern Sinai. *Petrol. Res. Bull.* 10, Government Press, Cairo, 154 pp.
- Morgan, P., Blackwell, D., Farris, J., Boulos, F. and Salib, P., 1977: Preliminary geothermal gradient and heat flow values for northern Egypt and the Gulf of Suez from oil well data. *Geotherm. Energy* 1, pp. 424-438.
- Morgan, P., Boulos, F., Hennin, S., El-Sheriff, A., Sayed, A., Basta N., and Melek, Y., 1985: Heat flow in eastern Egypt: The thermal signature of a continental breakup. *J. Geodyn.* 4, pp. 107-131.
- Okubo, Y., Graf, R.J., Hansent, R. O., Ogawa, K. and Tsu, H. (1985). Curie point depths of the island of Kyushu and surrounding areas Japan. *Geophysics*, Vol.53, pp.481-494.

- Omara, S., 1972: An early Cambrian outcrop in southwestern Sinai, Egypt. N.J.P. Geol.Palaeontol. 5, 306-314.
- Reid, A.B., Allsop, J.M., Granser, H., Millett, A.J., Somerton, I.W., 1990. Magnetic interpretation in three dimensions using Euler deconvolution. *Geophysics* 55, 80-9
- Said, R., 1962: The geology of Egypt. Elsevier, Amsterdam-New York, pp.1-377.
- Said, R., 1990: The Geology of Egypt. Balkema: Rotterdam, 734p.
- Salem, A., Ushijima, K., Elsirafi, A., and Mizunaga, H., 2000: Spectral analysis of aeromagnetic data for geothermal reconnaissance of Quseir area, northern Red Sea, Egypt. Proceeding World Geothermal Congress. 1969-1674.
- Shata, A. 1956. Structural development of Sinai Peninsula, Egypt. *Bulletin Institut Desert Egypt* 6, 117-157.
- Shuey, R.T., Schellinger, D.K., Tripp, A.C., and Alley, L.B. (1977). Curie depth determination from aeromagnetic spectra. *Geophys. J. the Roy. Astr. Soc.*, Vol.50,pp.75-101.
- Steckler, M., 1985: Uplift and extension at the Gulf of Suez- indication of induced mantle convection. *Nature*, 317, 135-139.
- Swanberg, C., Morgan, P., and Boulos, F., 1983: Geothermal potential of Egypt. *Tectonophysics*, 96, 77-94.
- Tewfic, R., 1975: Geothermal gradients in the Gulf of Suez. Internal report, Gulf of Suez Oil Co., Cairo.
- Thompson, D.T., 1982. EULDPH: a new technique for making computer-assisted depth estimates from magnetic data. *Geophysics* 47, 31-37.
- Uchida, T., 1991: 2D resistivity inversion for Schlumberger sounding. *Butsuri -Tansa* Vol.44 No.1, 1-17.
- Zohdy, A., 1989: A new method for the automatic interpretation of Schlumberger and Wenner Sounding curves. *Geophysics* Vol.54 No.2, 245-253.